END
DATE
FILMED
12-81
DTIC

LEVEL 1 (12)

REPORT DOCUMENTATION PAGE		READ INSTRUCTIONS BEFORE COMPLETING FORM
1. REPORT NUMBER ONR-TR-30 - ETIR	2. GOVT ACCESSION NO. AD-A106 928	3. RECIPIENT'S CATALOG NUMBER
4. TITLE (and Subtitle) Electrostatic Binding of Electroactive and Non-electroactive Anions in a Surface-Confined, Electroactive Polymer: Selectivity of Binding Measured by Auger Spectroscopy and Cyclic Voltammetry		5. TYPE OF REPORT & PERIOD COVERED Interim Technical Report
		6. PERFORMING ORG. REPORT NUMBER
7. AUTHOR(s) James A. Bruce and Mark S. Wrighton		8. CONTRACT OR GRANT NUMBER(s) N00014-75-C-0880
9. PERFORMING ORGANIZATION NAME AND ADDRESS Department of Chemistry Massachusetts Institute of Technology Cambridge, Massachusetts 02139		10. PROGRAM ELEMENT, PROJECT, TASK AREA & WORK UNIT NUMBERS NR 051-579
11. CONTROLLING OFFICE NAME AND ADDRESS Office of Naval Research Department of the Navy Arlington, Virginia 22217		12. REPORT DATE Sept 15 1981
		13. NUMBER OF PAGES 48
14. MONITORING AGENCY NAME & ADDRESS(if different from Controlling Office)		15. SECURITY CLASS. (of this report) Unclassified
		15a. DECLASSIFICATION/DOWNGRADING SCHEDULE

16. DISTRIBUTION STATEMENT (of this Report)

Approved for public release; reproduction is permitted for any purpose

of the United States Government; distribution unlimited.

17. DISTRIBUTION STATEMENT (of the abstract entered in Block 20, if different from Report)

Distribution of this document is unlimited.

DTIC
SELECTE
OCT 0 1 1981
E

18. SUPPLEMENTARY NOTES

19. KEY WORDS (Continue on reverse side if necessary and identify by block number)

20. ABSTRACT (Continue on reverse side if necessary and identify by block number)

PLEASE TURN OVER FOR ABSTRACT

Electrodes can be functionalized with {N,N'-Bis(-3-(trimethoxysilyl)propyl)-4,4'-bipyridinium}dibromide, I, yielding a surface-confined, electroactive polymer, $(PQ^{2+} \cdot 2Br^-)_n$. The anions are labile and can be replaced readily by a number of anions. By a combination of Auger and electrochemical techniques we have studied the incorporation of the anions: p-toluenesulfonate, Cl^-, Br^-, I^-, ClO_4^-, SCN^-, SO_4^{2-}, $Fe(CN)_6^{4-}$, $Ru(CN)_6^{4-}$, $Co(CN)_6^{3-}$, $Mo(CN)_8^{4-}$, $IrCl_6^{2-}$, and $PtCl_6^{2-}$ into $(PQ^{2+})_n$. Generally, the transition metal complex anions are more firmly bound and less labile than the other anions. The ordering of monoanions is p-toluenesulfonate $\approx Cl^- < Br^- \approx ClO_4^- \approx SCN^- < I^-$. The SO_4^{2-} anion competes well with ClO_4^- and not as well with I^-. For the monoanions and SO_4^{2-} the selectivity for binding spans a range of apprxoimately an order of magnitude. For example, a solution having 0.09 $\underline{M}$ Cl^- and 0.01 $\underline{M}$ I^- has ~50% I^- and ~50% Cl^- in the $(PQ^{2+})_n$. The selectivity for binding $IrCl_6^{2-}$, the most weakly bound transition metal complex, is considerable. For example, a solution having 0.1 $\underline{M}$ SO_4^{2-} and 5 x 10^{-5} $\underline{M}$ $IrCl_6^{2-}$ gives >50% $IrCl_6^{2-}$ in the $(PQ^{2+})_n$ when analyzed by Auger spectroscopy after removal from the solution followed by washing. The complexes $Mo(CN)_8^{4-}$, $Fe(CN)_6^{4-}$, $Ru(CN)_6^{4-}$, and $IrCl_6^{2-}$ exhibit chemically reversible redox reaction when bound to the polymer, as determined by cyclic voltammetry. Such electroactive anions can be bound in the $(PQ^{2+})_n$ polymer for prolonged periods (>1 h) in the presence of 0.1 $\underline{M}$ KCl. Cyclic voltammetry of electrodes having variable amounts of $IrCl_6^{3-}$.
$(PQ^{2+} \cdot \frac{2}{3} x \ IrCl_6^{3-} + (1 - x)SO_4^{2-})_n$ (x = 0-1), correlates well with intensity of Auger signals characteristic of $IrCl_6^{3-}$ relative to those for $(PQ^{2+})_n$, providing confidence in our use of Auger to order the binding of nonelectroactive anions. Electrochemistry allows an ordering of $IrCl_6^{2-} < Fe(CN)_6^{4-} \approx Ru(CN)_6^{4-} <$ $Mo(CN)_8^{4-}$ for the electroactive ions. The effect of $Co(CN)_6^{3-}$ on the electrochemistry of $Fe(CN)_6^4$ and $Mo(CN)_8^{4-}$ places $Co(CN)_6^{3-}$ near $Ru(CN)_6^{4-}$ in this ordering.

OFFICE OF NAVAL RESEARCH

CONTRACT N00014-75-C-0880

Task No. NR 051-579

TECHNICAL REPORT NO. 30

"ELECTROSTATIC BINDING OF ELECTROACTIVE AND NONELECTROACTIVE

ANIONS IN A SURFACE-CONFINED ELECTROACTIVE POLYMER:

SELECTIVITY OF BINDING MEASURED BY AUGER SPECTROSCOPY AND CYCLIC VOLTAMMETRY"

by

James A. Bruce and Mark S. Wrighton

Department of Chemistry
Massachusetts Institute of Technology
Cambridge, Massachusetts 02139

September 15, 1981

Electrostatic Binding of Electroactive and Nonelectroactive Anions in a

Surface-Confined, Electroactive Polymer: Selectivity of Binding Measured

by Auger Spectroscopy and Cyclic Voltammetry

James A. Bruce and Mark S. Wrighton[*]

Department of Chemistry
Massachusetts Institute of Technology
Cambridge, Massachusetts 02139 U.S.A.

Abstract: Electrodes can be functionalized with {N,N'-Bis(-3-(trimethoxy-silyl)propyl)-4,4'-bipyridinium}dibromide, I, yielding a surface-confined, electroactive polymer, $(PQ^{2+} \cdot 2Br^-)_n$. The anions are labile and can be replaced readily by a number of anions. By a combination of Auger and electrochemical techniques we have studied the incorporation of the anions: p-toluenesulfonate, Cl^-, Br^-, I^-, ClO_4^-, SCN^-, SO_4^{2-}, $Fe(CN)_6^{4-}$, $Ru(CN)_6^{4-}$, $Co(CN)_6^{3-}$, $Mo(CN)_8^{4-}$, $IrCl_6^{2-}$, and $PtCl_6^{2-}$ into $(PQ^{2+})_n$. Generally, the transition metal complex anions are more firmly bound and less labile than the other anions. The ordering of monoanions is p-toluenesulfonate $\approx Cl^- < Br^- \approx ClO_4^- \approx SCN^- < I^-$. The SO_4^{2-} anion competes well with ClO_4^- and not as well with I^-. For the monoanions and SO_4^{2-} the selectivity for binding spans a range of approximately an order of magnitude. For example, a solution having $0.09\underline{M}\ Cl^-$ and $0.01\ \underline{M}\ I^-$ has ~50% I^- and ~50% Cl^- in the $(PQ^{2+})_n$. The selectivity for binding $IrCl_6^{2-}$, the most weakly bound transition metal complex, is considerable. For example, a solution having $0.1\ \underline{M}\ SO_4^{2-}$ and $5 \times 10^{-5}\ \underline{M}\ IrCl_6^{2-}$ gives >50% $IrCl_6^{2-}$ in the $(PQ^{2+})_n$ when analyzed by Auger spectroscopy after removal from the solution followed by washing. The complexes $Mo(CN)_8^{4-}$, $Fe(CN)_6^{4-}$, $Ru(CN)_6^{4-}$, and $IrCl_6^{2-}$ exhibit chemically reversible redox reaction when bound to the polymer, as determined by cyclic voltammetry. Such electroactive anions can be bound in the $(PQ^{2+})_n$ polymer for prolonged periods (>1 h) in the presence of $0.1\ \underline{M}\ KCl$. Cyclic voltammetry of electrodes having variable amounts of $IrCl_6^{3-}$, $(PQ^{2+} \cdot \frac{2}{3}xIrCl_6^{3-} + (1-x)SO_4^{2-})_n$ (x = 0-1), correlates well with intensity of Auger signals characteristic of $IrCl_6^{3-}$ relative to those for $(PQ^{2+})_n$, providing confidence in our use of Auger to order the binding of nonelectroactive anions. Electrochemistry allows an ordering of $IrCl_6^{2-} < Fe(CN)_6^{4-} \approx Ru(CN)_6^{4-} < Mo(CN)_8^{4-}$ for the electroactive ions. The effect of $Co(CN)_6^{3-}$ on the electrochemistry of $Fe(CN)_6^4$ and $Mo(CN)_8^{4-}$ places $Co(CN)_6^{3-}$ near $Ru(CN)_6^{4-}$ in this ordering.
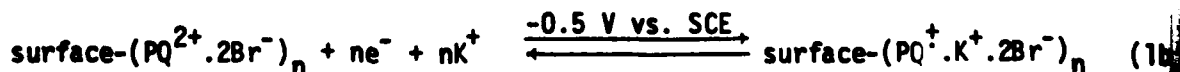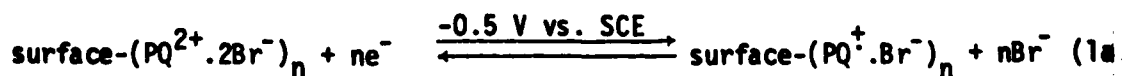
Electrodes derivatized with electroactive polymers or with charged, nonelectroactive polymers can be significantly influenced by the nature of the electrolyte and other ions present in a solution contacted by the derivatized electrode. It has been shown that charged, nonelectroactive polymers can persistently bind significant quantities of charged, electroactive species such as $Fe(CN)_6^{4-}$ by surface polyvinylpyridinium[1-3] or $Ru(bipyridine)_3^{2+}$ by Nafion.[4] These examples illustrate how electrostatic binding may be exploited for analysis, preparation of a variety of modified electrodes, and study of electrocatalysis. Electroactive polymers are charged in at least one of their accessible redox states and both selectivity of counterion binding and the movement of ions in and out of the surface polymer associated with change of redox state may affect electrochemical behavior.[5-7] Electrodes coated with electroactive polymers may have a number of uses,[8] including desalting of H_2O,[9] that depend on the behavior of solution ions.

Recent work in this laboratory[10,11] has involved the use of reagent I

$$\left[(MeO)_3Si-(CH_2)_3-N\underset{\bigcirc}{\bigcirc}-\underset{\bigcirc}{\bigcirc}N^+-(CH_2)_3-Si(OMe)_3 \right]^{2+} 2\,Br^-$$
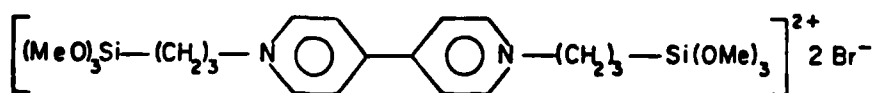
I

to functionalize photocathode surfaces yielding a surface-confined electroactive polymer, $(PQ^{2+}.2Br^-)_n$. The ability to observe essentially reversible redox chemistry for the $(PQ^{2+})_n$ in aqueous KBr suggests good mobility for the anions, equation (1a) and/or the cations, equation (1b).

$$\text{surface-}(PQ^{2+}.2Br^-)_n + ne^- \xrightarrow[\longleftarrow]{-0.5\ V\ vs.\ SCE} \text{surface-}(PQ^+.Br^-)_n + nBr^- \quad (1a)$$

$$\text{surface-}(PQ^{2+}.2Br^-)_n + ne^- + nK^+ \xrightarrow[\longleftarrow]{-0.5\ V\ vs.\ SCE} \text{surface-}(PQ^+.K^+.2Br^-)_n \quad (1b)$$

We exploited the lability of the anions to incorporate Pt(0) in the polymer as a hydrogen evolution catalyst,[11] equations (2) and (3). In this

$$\text{surface-}(PQ^{2+}.2Br^-)_n + nK_2PtCl_6 \rightarrow \text{surface-}(PQ^{2+}.PtCl_6^{2-})_n + 2nKBr \quad (2)$$

$$\text{surface-}(PQ^{2+}.PtCl_6^{2-})_n \xrightarrow{\underset{KBr}{\text{reduce}}} \text{surface-}(PQ^{2+}.2Br^-/Pt(0))_n + 6nCl^- \quad (3)$$
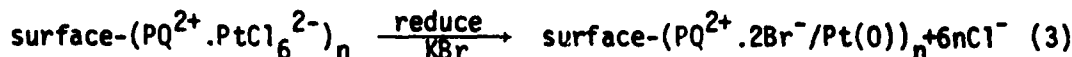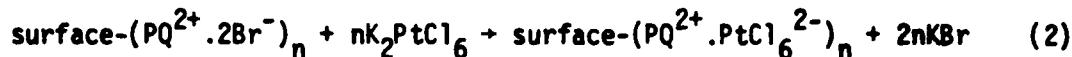
article we put our preliminary results for $PtCl_6^{2-}$ incorporation on a quantitative footing and amplify our studies of ion exchange involving both electroactive and nonelectroactive anions. Of particular importance is the establishment of Auger spectroscopy as a good tool for determining the presence, and relative amount, of ions such as Cl^-, Br^-, etc. that are difficult to determine by other techniques. It has been claimed that X-ray photoelectron spectroscopy is a useful technique to detect such anions on modified electrode surfaces.[12] The electrodes that have been studied are Pt and p-type Si,[11] but the results should be directly extendable to any other surface modified with I.

Experimental

Electrodes and Derivatization. Single crystal p-Si wafers (0.35 mm thick,
(111) face exposed) doped with B (resistivity, 3-7 ohm-cm), were obtained
from Monsanto Co., Electronics Division (Palo Alto, CA). Ohmic contact to
the back of the electrode was made by vapor deposition of Al then sintering
at 723 K under N_2 for 5 min. Electrodes were mounted as previously described.[10,11]
Typical electrode areas ranged from 10-25 mm^2.

Synthesis of $\underline{I}$ has been previously described.[10,11] For derivatization of
Si, the Si electrodes are first etched in concentrated HF at 298 K for 60 s
then rinsed in distilled H_2O and dipped in 10 $\underline{M}$ NaOH at 298 K for 60 s. The
electrode is then rinsed again in distilled H_2O, followed by acetone and air
dried. The electrodes are then immersed into a 1-5 m$\underline{M}$ solution of $\underline{I}$ in CH_3CN
under N_2 and left for 3-48 hrs at 298 K. After removal from solution, the
electrodes are rinsed with CH_3CN and stored under Ar. Pt foil electrodes are
electrochemically pretreated as previously described.[13] Pt electrodes were
then derivatized with $\underline{I}$ either by immersion into 1-5 m$\underline{M}$ solutions of $\underline{I}$ in CH_3CN,
or by potentiostatting the electrodes at -0.72 V vs. SCE in aqueous 0.1 $\underline{M}$ K_2HPO_4,
0.2 $\underline{M}$ KCl, ~3 m$\underline{M}$ $\underline{I}$. Coverage of electroactive $(PQ^{2+})_n$ was determined by
integration of the cyclic voltammetric wave associated with $(PQ^{2+})_n \rightleftarrows (PQ^{+})_n$

Electrochemical Equipment. Cyclic voltammograms were obtained using a PAR model
173 potentiostat, a model 175 programmer, and a Houston Instruments 2000 XY
recorder. All experiments were performed in a single compartment Pyrex cell
equipped with a saturated calomel reference electrode (SCE), a Pt wire counter-
electrode, and a Pt or p-Si working electrode. The solution contained 0.1 $\underline{M}$
supporting electrolyte. Reagent grade chemicals and distilled, deionized
H_2O were used. Studies involving electrodes derivatized with $\underline{I}$ were carried
out under Ar. P-Si electrodes were illuminated with a beam expanded 632.8 nm
He-Ne laser (Aerotech or Coherent Radiation) providing up to ~50 mW/cm^2.

Ion Exchange Into $(PQ^{2+})_n$ Polymer. Replacing the Br^- in $(PQ^{2+} \cdot 2Br^-)_n$ by another anion was accomplished by placing the electrode into an aqueous solution of the appropriate ions. The electrode was then left to equilibrate at 298 K for a period of time long enough to insure that equilibrium was established. The electrode was then well-rinsed with distilled, deionized H_2O to remove any excess electrolyte.
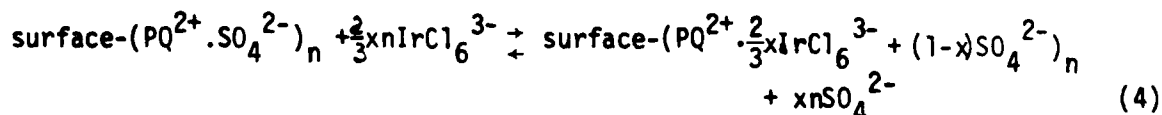
Auger Spectroscopy. Auger spectra were obtained on a Physical Electronics Model 590A scanning Auger spectrometer. A 5 keV electron beam with a beam current of from 0.3 to 1 μA was used as the excitation source. Si samples were mounted by attaching the Cu wire lead to the sample holder, and Pt samples were clipped down to insure electrical grounding. The pressure was maintained at $<10^{-8}$ torr during analysis. A 3 keV electron beam was used in a few samples where charging was a problem.

Depth profiling using an Auger spectrometer has been previously described.[14] A Physical Electronics Model 04-303 differential ion gun was used to produce a 2 keV Ar^+ ion beam for sputtering. The pressure was maintained at ~3 x 10^{-7} torr in the main vacuum chamber, and 1.5 x 10^{-4} torr of Ar in the ionization chamber. Generally, signals for C, N, O, Si, the counterion of $(PQ^{2+})_n$, and the substrate (Si or Pt) were analyzed as a function of sputtering time.[15] The energy window used was typically 10-50 eV around the energy characteristic of the element being analyzed. The Auger signals (and their energies) monitored during depth profiles are as follows: C (273 eV); N (379 eV); O (503 eV); Cl (181 eV); S (152 eV); Si (1619 eV); Br (1396 eV); I (511 and 520 eV); and Pt (1967 eV).

Results and Discussion

a. Correlation of Auger Spectroscopic and Electrochemical Analysis of Electrostatically Bound Anions: Binding of $IrCl_6^{2-}$.

Pt electrodes bearing $\sim 10^{-8}$ mol/cm^2 of $(PQ^{2+}.2Br^-)$ exhibit essentially reversible reduction of the $(PQ^{2+})_n$ at -0.5 V vs. SCE in 0.1 $\underline{M}$ K_2SO_4 solution. If K_2IrCl_6 is introduced into the solution an additional redox system is detectable by cyclic voltammetry at $\sim +0.6$ V vs. SCE that is attributable to the $IrCl_6^{2-/3-}$ redox couple. At concentrations of $IrCl_6^{2-}$ where no $IrCl_6^{2-/3-}$ cyclic voltammetry wave is detectable for a naked electrode (1-50 $\mu\underline{M}$) we observe a wave for electrodes bearing $\sim 10^{-8}$ mole/cm^2 of PQ^{2+}. We thus conclude, as was concludec previously for polyvinylpyridinium,[1-3] that the $(PQ^{2+})_n$ can electrostatically bind $IrCl_6^{2-}$ resulting in an electrochemical response that woula otherwise be undetectable. Figure 1 shows cyclic voltammograms for five different electrodes bearing about the same amount of $(PQ^{2+})_n$ in 0.1 $\underline{M}$ K_2SO_4 solution but with a different concentration of $IrCl_6^{2-}$ in solution in each case. The signal for $IrCl_6^{2-} \rightleftarrows IrCl_6^{3-}$ grows from zero to the value shown in 10-15 min. The data in Figure 1 are representative for this system and are believed to reflect the equilibrium amount of $IrCl_6^{3-}$ electrostatically bound in $(PQ^{2+})_n$. While $IrCl_6^{2-}$ is present in the bulk, the species actually bound is $IrCl_6^{3-}$ because the electrodes were held at a potential suffi-ciently negative to reduce the $IrCl_6^{2-}$. Thus, equation (4) represents the ion

$$\text{surface-}(PQ^{2+}.SO_4^{2-})_n + \tfrac{2}{3}xnIrCl_6^{3-} \rightleftarrows \text{surface-}(PQ^{2+}.\tfrac{2}{3}xIrCl_6^{3-} + (1-x)SO_4^{2-})_n + xnSO_4^{2-} \quad (4)$$

exchange reaction. By integrating the cyclic voltammetry waves the value of x is determined to vary from ~ 0.1 up to ~ 1.0, Table I, depending on the bulk concentration of $IrCl_6^{2-}$. At very low concentrations of $IrCl_6^{2-}$ there might be some concern as to whether there is significant depletion of the bulk $IrCl_6^{2-}$. For ~ 25 ml solutions of the 1 $\mu\underline{M}$ $IrCl_6^{2-}$ there is a total reservoir of ~ 25 nmoles of $IrCl_6^{2-}$; for $x = 1.0$ this would represent a diminution in the reservoir of $IrCl_6^{2-}$ by less than 25%, since the electrode bears only 7.6 nmoles of PQ^{2+}. That the amount of $IrCl_6^{3-}$ in the electrode is the equilibrium amount is established by showing

that an electrode where $x = 1.0$ initially changes in time to a value consistent with the bulk $IrCl_6^{2-}$ concentration associated with the solution contacting the electrode. Thus, the same eventual amount of $IrCl_6$ attained at given bulk concentration of $IrCl_6^{2-}$, independent of the initial value of x, for a fixed K_2SO_4 concentration. The timescale of the equilibration, however, can be quite long, requiring >15 min. in some cases.

Two, more subtle, observations tend to confirm the conclusion that $SO_4^{2-}/IrCl_6^{2-/3-}$ equilibration does occur. First, note that $IrCl_6^{2-}$ can be introduced as the 2- species by not potentiostatting the electrode. In the 50 $\underline{\mu M}$ $IrCl_6^{2-}$ solution we find that the area under the wave for $IrCl_6^{2-} \rightleftarrows IrCl_6^{3-}$ is initially very close to that under the wave for $(PQ^{2+})_n \rightleftarrows (PQ^{+\cdot})_n$, when the non-potentiostatted electrode is equilibrated with the solution. However, holding the electrode between $E°(PQ^{2+/+\cdot})_n$ and $E°(IrCl_6^{2-/3-})$ for a few minutes and then scanning to determine the amount of surface-confined $IrCl_6^{2-} \rightleftarrows IrCl_6^{3-}$ reveals a diminution in the area under the wave for $IrCl_6^{2-} \rightleftarrows IrCl_6^{3-}$ to a value consistent with the binding of $IrCl_6^{3-}$ to an extent that the positive charge of the $(PQ^{2+})_n$ is fully compensated. It is reasonable that if $IrCl_6^{2-}$ is bound to the fullest extent at 50 $\underline{\mu M}$ then $IrCl_6^{3-}$ would be bound just as well, if not better, since it bears a higher negative charge. The second observation concerns the effect from putting a $Pt/(PQ^{2+} \cdot \frac{2}{3}IrCl_6^{3-})_n$ electrode at a potential of $--0.65$ V vs. SCE, where the surface-$(PQ^{2+})_n$ is put in the reduced state $(PQ^{+\cdot})_n$, in a solution containing 50 $\underline{\mu M}$ $IrCl_6^{2-}$. The first several scans to determine surface $IrCl_6^{3-}$ show the approximately 50% diminution of the signal for $IrCl_6^{2-} \rightleftarrows IrCl_6^{3-}$ expected from the reduction in positive charge of the polymer. These two experiments show that $IrCl_6^{2-/3-}$ can move in and out of the $(PQ^{2+})_n$ layer with sufficient facility that equilibrium with the solution ions can be established.

Two additional points should be made here. First, the cyclic voltammetry is not useful in establishing whether there is additional electrolyte in the surface layer beyond that associated with charge compensation of the $(PQ^{2+})_n$. For example, there may be K_2SO_4 present in the polymer layer. Since reasonable electrochemical responses are observed for the $(PQ^{2+/+\cdot})_n$ and for surface-confined $IrCl_6^{2-/3-}$, the presence of H_2O in the polymer layer is certain. But whether K_2SO_4 is present in the layer is unclear. It is unlikely that excess electrolyte can be excluded, and indeed it may be that K^+ and SO_4^{2-} are the most mobile ions when there is as much $IrCl_6^{2-/3-}$ as PQ^{2+} in the polymer layer. In any event, the local concentration of ions in the polymer layer far exceeds the bulk concentration even when the bulk concentration of electrolyte is 0.1 $\underline{M}$. In the absence of a firmly bound anion such as $IrCl_6^{3-}$, the supporting electrolyte charge compensates the polymer thereby enhancing the electrolyte concentration near the electrode. When a firmly bound anion is present the concentration of supporting electrolyte may in fact be smaller than in solution, but the total ion concentration in the region near the electrode is always higher when the polymer is present. The second point of importance is that the extent to which $IrCl_6^{2-/3-}$ will be present in the surface polymer depends on the other ions present in the solution. This will be elaborated more fully below but it should be noted here that there are more and less competitive anions than SO_4^{2-}.

The electrodes characterized by the data in Figure 1 and Table I were studied further by Auger spectroscopy, to establish a quantitative correlation between the electrochemically detected $IrCl_6^{2-/3-}$ and Auger signals characteristic of the $IrCl_6^{2-/3-}$. Electrodes were removed from the solutions containing the various $IrCl_6^{2-}$ concentrations and washed with distilled, deionized H_2O. The five electrodes having variable $IrCl_6^{3-}$ content presumably have the surface$(PQ^{2+} \cdot \frac{2}{3}xIrCl_6^{3-} \cdot (1-x)SO_4^{2-})$ composition present

in the electrolyte solution from which each was withdrawn, except for the complication of the unknown K_2SO_4 content. The Auger spectra of the electrodes show signals for C, N, Si, and O, that are expected for $(PQ^{2+})_n$, Figure 2, and additional signals are present in the spectrum that are attributable to the elements S (from SO_4^{2-}) and Ir and Cl (from $IrCl_6^{3-}$) depending on the solution from which the surface is withdrawn. No additional signals are observed, and in particular, we find little or no detectable signal for K (252 eV) (from K^+). Any K_2SO_4 in the polymer is likely washed away during rinsing with H_2O following removal from the K_2IrCl_6/K_2SO_4 solution. For each electrode the ratio of the N signal to the C signal is the same, ±20%, but the Cl to C ratio varies in a smooth fashion depending on the concentration of $IrCl_6^{2-}$ in the solution from which the electrode was withdrawn, Figure 3. The correlation in Figure 3 is also with the data in Figure 1 that gives the ratio of electroactive, surface-confined $PQ^{2+/+}$ and $IrCl_6^{2-/3-}$. As shown in Figure 3 there is excellent internal consistency between the in situ electrochemical determination of $IrCl_6^{2-/3-}$ and the Auger determination of a washed and dried surface taken from the electrolyte solution. Thus, we can associate particular Cl/C ratios from Auger with a particular fractional incorporation of electroactive $IrCl_6^{3-/2-}$.

In our earlier work[11] we showed by Auger that the replacement of Br^- by Cl^- according to equation (5) occurs to an extent that no Br^- is detectable

$$(PQ^{2+}.2Br^-)_n \xrightarrow[\text{Aqueous KCl}]{} (PQ^{2+}.2Cl^-)_n + 2nKBr \qquad (5)$$
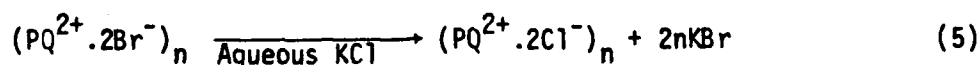
by Auger spectroscopy. For such a surface the Cl/C ratio is less than for $(PQ^{2+}.PtCl_6^{2-})_n$ by an amount that about reflects the factor of three lower Cl content. The Cl/C ratio for an electrode prepared according to equation (6) likewise is about a factor of three greater than for

$$(PQ^{2+}.2Br^-)_n \xrightarrow[\text{5 m\underline{M} } K_2IrCl_6]{} (PQ^{2+}.IrCl_6^{2-})_n + 2nKBr \qquad (6)$$
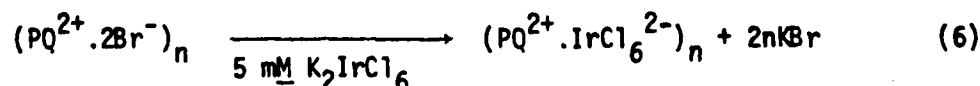
surface-$(PQ^{2+}.2Cl^-)_n$. The difference with the $IrCl_6^{2-}$ is that we can know the amount of electroactive $IrCl_6^{2-/3-}$ that is present, in contrast to $PtCl_6^{2-}$

which does not exhibit reversible electrochemistry. Since the $IrCl_6^{2-}$ is very similar to $PtCl_6^{2-}$ in size and charge, the behavior of $IrCl_6^{2-}$ is expected to be close to that for $PtCl_6^{2-}$ in terms of incorporation into $(PQ^{2+})_n$ when competing against other anions.

Auger spectroscopic analysis of electrode surfaces bearing $(PQ^{2+})_n$ and the charge compensating anions reveal the surfaces to be reasonably free of detectable contaminants. At least we do not observe signals for extraneous elements and the elements that are expected to be present are detectable. One additional check of internal consistency comes from monitoring the Auger signal intensity for the various detectable elements while sputtering away the exposed surface with a beam of reactive Ar ions. This so-called depth profile analysis gives information concerning the elemental composition of the electrode/polymer interface as a function of depth in the polymer. A typical set of depth profile analyses are given in Figure 4. Note that substrate Pt signals overlap those for N; Si and N are low sensitivity elements. These facts account for the nearly independent signal intensity for N and Si as a function of sputtering time. Generally, there is some variation in element ratios near the surface, as detected by the changing Auger signal intensity as the sputtering time increases. But within a short time, it would appear that the polymer layer, bearing different anions, does have constant composition. The Auger signal intensities without sputtering may thus be suspect, since these may not always accurately reflect the composition of the bulk of the polymer. On the other hand, the sputtering technique itself is a destructive one and can lead to selective removal of various substances as the surface suffers damage from both the Auger exciting beam and the Ar ion sputtering beam.[16] We generally find good qualitative agreement for Auger with and without sputtering in the sense that selective anion binding can be determined to occur, Figures 2 and 4. However, as is well appreciated by other workers using Auger spectroscopy, the quantitative determination of element ratios by Auger spectroscopy will not be as good as an elemental analysis from combustion analyses. We find very reasonable reproducibility and would

estimate an error of less than $\pm 30\%$ in determining the ratio of compensating anions in $(PQ^{2+})_n$ when taking ratios from depth profile analyses.

b. Electrostatic Binding of Electroactive Transition Metal Cyanide Complexes.

The incorporation of the electroactive $IrCl_6^{2-/3-}$ system into $(PQ^{2+})_n$ prompted us to examine the electrostatic binding of other negatively charged metal complexes. One large class of such complexes are the transition metal cyanides, a number of which can in fact be isolated in at least two oxidation states. We have thus examined the behavior of $Co(CN)_6^{3-}$, $Fe(CN)_6^{3-}$, $Fe(CN)_6^{4-}$, $Ru(CN)_6^{4-}$, and $Mo(CN)_8^{4-}$ as representative of this class. Of these, only $Co(CN)_6^{3-}$ does not exhibit reversible electrochemical behavior.

The metal cyanide complexes bind strongly to the $(PQ^{2+})_n$. Figure 5 shows typical electrochemical behavior of Pt electrodes derivatized with $\underset{\sim}{1}$ before and after incorporation of $Fe(CN)_6^{4-}$ or $Mo(CN)_8^{4-}$. Incorporation of the metal complex was brought about by dipping the unpotentiostatted $(PQ^{2+} \cdot 2Br^-)_n$ coated electrodes into an aqueous ~ 5 m$\underline{M}$ solution of the appropriate complex as the K^+ salt for ~ 5 min. The electrode was then removed, washed, and re-examined by cyclic voltammetry in 0.1 $\underline{M}$ KCl to determine whether any electroactive complex was retained. As shown in Figure 4 cyclic voltammetry waves having an area of $\sim \frac{1}{2}$ of that for the $(PQ^{2+})_n \rightleftarrows (PQ^+)_n$ are initially observed after replacement of Cl^- by $Mo(CN)_8^{4-}$ or $Fe(CN)_6^{4-}$. This $\sim 1:2$ ratio is that expected for complete compensation of charge by the complexes. The waves for the electrostatically bound anions do diminish with time in 0.1 $\underline{M}$ KCl, but even after 4 h detectable waves still obtain. For finite volumes of electrolyte solution it is apparent that there can be measurable amounts of the complex anions that persist in the polymer at equilibrium.

As for electrodes bearing $(PQ^{2+})_n$ into which $IrCl_6^{2-}$ is incorporated, Figure 4, we have recorded Auger spectra for unpotentiostatted Pt electrodes bearing $(PQ^{2+})_n$ that have been withdrawn, and subsequently washed, from solutions containing variable amounts of $K_4Fe(CN)_6$ and a fixed concentration of KCl. Auger spectra for a pair of electrodes are given in Figure 6. As expected, the Cl

signal associated with the $(PQ^{2+}.2Cl^-)_n$ is attenuated for the electrode

withdrawn from the solution containing the higher $Fe(CN)_6^{4-}$ concentration.

When incorporated, Figure 6b, $Fe(CN)_6^{4-}$ bound to the $(PQ^{2+})_n$ exhibits a signal

characteristic of Fe. Moreover, there is a definite change in the ratio of

the C/N ratio in accord with a high relative N concentration in

$(PQ^{2+}.\frac{1}{2}Fe(CN)_6^{4-})_n$ compared to $(PQ^{2+}.2Cl^-)_n$. The data in Figure 6 provide

further substantiation of the Auger spectroscopic technique as a method to

determine the relative binding of one anion compared to another. For all

of the transition metal complexes that we have investigated,

MCl_6^{2-} (M = Pt, Ir); $M(CN)_z^{n-}$ (M = Co, Fe, Ru, Mo), we find that only small

concentrations are required to completely displace the small inorganic anions

such as X^- (X = Cl, Br, I, NCS, ClO_4) or SO_4^{2-} from the $(PQ^{2+})_n$ on the

surface, even when the small anions are present at significant

(~0.1 $\underline{M}$) bulk concentration. Auger and electrochemical measurements

have been employed to draw this conclusion. In the sections

c. and d. below, we detail the procedures for ordering the binding of the

anions.

The metal cyanides studied are not substitution labile and likely remain

intact upon binding to the $(PQ^{2+})_n$. We find that in aqueous 0.1 $\underline{M}$ KCl

the positions of the cyclic voltammetry waves are close to those found when the

complexes are examined at the naked electrode surfaces, Table II. Thus, like

the $IrCl_6^{2-/3-}$ system, the metal cyanides can be incorporated into the polymer

with relatively little perturbation of the electrochemistry. The kinetics for the surface-confined species have not been studied in detail, but Figure 7 shows the variation of the cyclic voltammograms for electrostatically bound $Mo(CN)_8^{4-}$, illustrating that the $Mo(CN)_8^{3-} \rightleftarrows Mo(CN)_8^{4-}$ process is sufficiently fast to give the expected linear response of peak current with scan rate up to 200 mV/s. Data represented by Figure 7 for $Mo(CN)_8^{3-/4-}$ are representative of that for the other electrostatically bound anions that are electroactive.

The effect of the anion on the electrochemical response of the $(PQ^{2+})_n \rightleftarrows (PQ^{\cdot +})_n$ system is quite noticeable, Figure 5. The tightly bound anions $(Co(CN)_6^{3-}$, $Fe(CN)_6^{3-/4-}$, $Ru(CN)_6^{3-/4-}$, $Mo(CN)_8^{3-/4-}$, and $IrCl_6^{2-/3-})$ tend to broaden the wave and shift the average position of the oxidation and reduction current peaks to somewhat more negative potentials. The kinetics for the $(PQ^{2+})_n \rightleftarrows (PQ^{\cdot +})_n$ are also worsened by the incorporation of the tightly bound anions as reflected in the appearance of the cyclic voltammograms at scan rates exceeding 100 mV/s: the peak-to-peak separation increases and the waves appear broader. It is interesting that the electrochemical response of the metal complex is as good as it is, while the kinetics of the $(PQ^{2+})_n$ system suffer upon incorporation of the anion.

The electrochemical behavior of Pt electrodes bearing species such as $(PQ^{2+}.\frac{1}{2}Fe(CN)_6^{4-})_n$ is, not unexpectedly, dependent on the solvent. Since $E^\circ(Fe(CN)_6^{3-/4-})$ is dependent on solvent,[17] we felt that this sensitivity to solvent could be exploited to reveal the solvent composition inside the polymer layer compared to the bulk. Changing the solvent from H_2O to CH_3CN does have a profound effect on both the behavior of the $(PQ^{2+})_n \rightleftarrows (PQ^{\cdot +})_n$ and $Fe(CN)_6^{3-} \rightleftarrows Fe(CN)_6^{4-}$ systems. The $Fe(CN)_6^{3-/4-}$ wave is shifted more negative, broadened, and like the $(PQ^{2+/\cdot +})_n$ wave appears to be reduced in total area. Similar effects are found for the $(PQ^{2+}.\frac{1}{2}Mo(CN)_8^{4-})_n$. The poor electrochemical response in CH_3CN is found with 0.1 M $[n-Bu_4N]ClO_4$, $LiClO_4$, or $[Et_4N]Cl$ as supporting electrolyte. In all cases it would appear that the solvation by CH_3CN is so poor that the electrochemical behavior

of the surface groups is drastically worse. Changing from H_2O to CH_3CN solvent for a system such as $(PQ^{2+} \cdot 2Cl^-)_n$ on Pt only modestly affects the electrochemical response of the $(PQ^{2+/+\cdot})_n$ at cyclic voltammetry scan rates of ~100 mV/s. It would thus appear that the deleterious effects from CH_3CN as solvent can be attributed to the tight ion pairing of $(PQ^{2+})_n$ with the large anionic complexes. Interestingly, it would appear that only small amounts of H_2O added to CH_3CN (<5% by volume) are required to essentially regenerate the electrochemical properties found in pure H_2O solvent. The $(PQ^{2+} \cdot \text{complex anion})_n$ may concentrate the H_2O beyond the bulk concentration, since H_2O may solvate the ion pairs much more strongly.

Since the complex anions are persistently electrostatically bound to $(PQ^{2+})_n$ in solutions of 0.1 $\underline{M}$ KCl that contain no added complex anion, it is logical to conclude that the rate of loss of the complex is slow and that there is only slow movement of the complex anions in and out of the $(PQ^{2+})_n$ as the electrode is cycled between $(PQ^{2+})_n$ and $(PQ^{\cdot+})_n$. In these situations the essential charge neutrality of the polymer layer must be brought about by the movement of the cations, say K^+, in and out of the layer. Thus, relatively fast $(PQ^{2+})_n \rightleftarrows (PQ^{\cdot+})_n$ interconversion or redox cycling of the complex anion may depend on the cation mobility when there are complex anions tightly bound to the $(PQ^{2+/+\cdot})_n$ layer. As for $IrCl_6^{2-/3-}$, though, holding the polymer layer in the reduced state, $(PQ^{\cdot+})_n$, will result in the eventual extrusion of the proper fraction of complex anion. A saturated solution of KCl will more rapidly lead to the dimunition of the electrochemical response of the electrostatically bound anion.

<u>c. Ordering the Binding of Complex Anions.</u> As indicated above, the transition metal complex anions are much more firmly bound than the simple inorganic anions. In this section we describe results establishing the relative ordering of complex anion binding to $(PQ^{2+})_n$. To illustrate the issue we can ask whether $IrCl_6^{2-}$ or $Fe(CN)_6^{4-}$ will be the charge compensating ion for $(PQ^{2+})_n$ when the solution contains both $IrCl_6^{2-}$ and $Fe(CN)_6^{4-}$. To answer such a question we exploit the fact that both ions are reversibly electro-active and examine the electrochemical response of a $(PQ^{2+})_n$-coated Pt electrode in a solution containing 0.1 $\underline{M}$ KCl, 50 $\mu\underline{M}$ K_2IrCl_6 and 50 $\mu\underline{M}$ $K_4Fe(CN)_6$. The potential range scanned is such that $(PQ^{2+})_n$ remains in the oxidized (2+) state. Initially, cyclic voltammetry waves are observed for the $Fe(CN)_6^{3-} \rightleftharpoons Fe(CN)_6^{4-}$ and for the $IrCl_6^{2-} \rightleftharpoons IrCl_6^{3-}$ systems. However, eventually the signal for the Ir system vanishes while the signal for the Fe system increases until the cyclic voltammetry shows that the charge associated with $(PQ^{2+})_n$ is completely neutralized by the electroactive $Fe(CN)_6^{4-}$. Thus, we conclude that both $IrCl_6^{2-}$ and $Fe(CN)_6^{4-}$ can quickly go into the polymer, but the thermodynamics are such that $Fe(CN)_6^{4-}$ is significantly more firmly bound. Likewise, examining the electrochemical response of a $(PQ^{2+})_n$-coated electrode after ~15 min equilibration in 0.1 $\underline{M}$ KCl, 50 $\mu\underline{M}$ K_2IrCl_6, and 50 $\mu\underline{M}$ $K_4Fe(CN)_6$ shows waves for only the $Fe(CN)_6^{3-/4-}$ couple.

Examination of the electrochemical response of a $(PQ^{2+})_n$-coated Pt electrode in 0.1 $\underline{M}$ KCl, 50 $\mu\underline{M}$ $K_4Fe(CN)_6$, 50 $\mu\underline{M}$ $K_4Mo(CN)_8$ initially reveals cyclic voltammetry signals for both the Fe and Mo systems. During the first few cyclic voltammetry scans the signal for the Fe and the Mo systems both grow, but the signal for Fe grows faster. This suggests that the $Fe(CN)_6^{4-}$ is more mobile than $Mo(CN)_8^{4-}$. Eventually, the signal for the Fe system declines while the Mo signal slowly grows to reflect a very high $Mo(CN)_8^{4-}/Fe(CN)_6^{4-}$ ratio bound to $(PQ^{2+})_n$. Similar experimentation shows that $Mo(CN)_8^{4-}$ is bound much more firmly than $Ru(CN)_6^{4-}$, while $Ru(CN)_6^{4-}$ is only slightly more firmly bound than $Fe(CN)_6^{4-}$.

The results from cyclic voltammetry of (PQ^{2+})-coated Pt electrodes in the presence of pairs of the electroactive complex anions allows us to establish the ordering of binding:

$$Mo(CN)_8^{4-} > Ru(CN)_6^{4-} \sim Fe(CN)_6^{4-} > IrCl_6^{2-/3-} \gg Cl^-$$
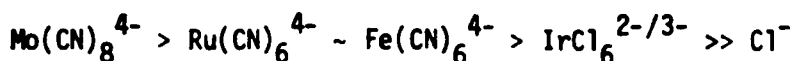
$\overleftarrow{}$
Increased Binding

Attenuation of the cyclic voltammetry wave for polymer-bound $Fe(CN)_6^{3-} \rightleftarrows Fe(CN)_6^{4-}$ by adding $K_3Co(CN)_6$ to a solution of 0.1 $\underline{M}$ KCl/50 $\mu\underline{M}$ $K_4Fe(CN)_6$ provides evidence for the strong and competitive binding of $Co(CN)_6^{3-}$ even though $Co(CN)_6^{3-}$ is electrochemically silent in the accessible potential range in H_2O. For example, addition of $K_3Co(CN)_6$ to bring its concentration to 25 $\mu\underline{M}$ attenuates the signal for the $Fe(CN)_6^{3-/4-}$ couple to ~50% of its initial value; addition of $K_3Co(CN)_6$ to a concentration of 50 $\mu\underline{M}$ attenuates the wave for $Fe(CN)_6^{3-/4-}$ even more, to about 30% of its original value. These experiments place $Co(CN)_6^{3-}$ in the vicinity of $Fe(CN)_6^{4-}$ and $Ru(CN)_6^{4-}$. However, $Co(CN)_6^{3-}$ is considerably more weakly bound than $Mo(CN)_8^{4-}$. This conclusion follows from the fact that $Mo(CN)_8^{4-}$ is the dominant polymer-bound electroactive ion when $(PQ^{2+})_n$-coated Pt electrodes are immersed in electrolyte solutions containing equal concentrations of $Fe(CN)_6^{4-}$ and $Mo(CN)_8^{4-}$, whereas $Fe(CN)_6^{4-}$ is still present at significant concentration in the $(PQ^{2+})_n$ when $Fe(CN)_6^{4-}$ and $Co(CN)_6^{3-}$ are in the bulk solution at equal concentration.

The same signal for the $Fe(CN)_6^{3-/4-}$ system is eventually observed if a $(PQ^{2+} \cdot 2Cl^-)_n$-coated electrode is immersed into a 0.1 $\underline{M}$ KCl solution that contains 50 $\mu\underline{M}$ $K_4Fe(CN)_6$ and 50 $\mu\underline{M}$ $K_3Co(CN)_6$ as when a $(PQ^{2+} \cdot \frac{1}{2}Fe(CN)_6^{4-})_n$ electrode is immersed into the same solution. The point is that the composition of the surface-bound polymer·anion system, $(PQ^{2+} \cdot xFe(CN)_6^{4-} \cdot yCo(CN)_6^{3-})_n$, is obtained independent of the initial composition of the electrode or the order of addition of reagents. The conclusion is that the $(PQ^{2+})_n$-coated Pt does come

into equilibrium with the ions in solution. Similarly, concerning the composition of the bound, electroactive anions $M(CN)_6^{4-}$ (M = Fe, Ru); $Mo(CN)_8^{4-}$; and $IrCl_6^{2-}$ the electrochemical response is eventually independent of the initial distribution of ions in the polymer, and the order of addition of anions to a solution does not alter the distribution of detected anions in the $(PQ^{2+})_n$ layer. Thus, in all cases, our measurements of anion binding are for situations where we are certain that equilibrium has been established; we are not limited by kinetically sluggish ion exchange. Table III summarizes the experimentation discussed so far to establish the ordering of the binding of complex anions, and Figures 8 and 9 illustrate typical cyclic voltammetry data for such experimentation. Comparison of wave shapes in Figures 1, 5, 7-9 indicate considerable variation. Such variation may be due to the differences in coverage, degree of cross-linking in the polymer, and the nature of the distribution of electroactive complex(es) present in the film.

Auger spectroscopy can also be used to order the binding of the tightly bound transition metal complexes, as illustrated by the spectra given in Figures 2 and 6. Generally, the unique Auger signal for the metal ion of the complex is weak and element ratios are not always easily quantitated. For example, the signal for Fe or Mo when the respective cyanide complexes are bound to $(PQ^{2+})_n$ is very weak relative to the signal for C. Consequently, we have not used Auger to order binding of the tightly bound, electroactive metal complexes.

d. Ordering the Binding of Weakly Bound, Non-Electroactive Anions. Table IV details Auger spectroscopy results that allow us to order the binding of several anions to the $(PQ^{2+})_n$. A typical experiment involves dipping a $Pt/(PQ^{2+}\cdot 2Br^-)_n$ electrode into an aqueous solution containing a one-to-one ratio of two anions. Equilibration at 25°C for 15 min is generally sufficient to insure that the anions in the polymer reflect the equilibrium situation. The equilibrated surface is then removed from the solution, washed with distilled H_2O, and then analyzed for the anion by Auger/depth profile analysis.

The series of experiments summarized by the data in Table IV allow the ordering of anions:

$$I^- > SCN^- \sim ClO_4^- \sim SO_4^{2-} > Br^- > Cl^- \sim \underline{p}\text{-toluenesulfonate}$$
$$\xleftarrow{\hspace{3cm}}$$
$$\text{increasing binding}$$
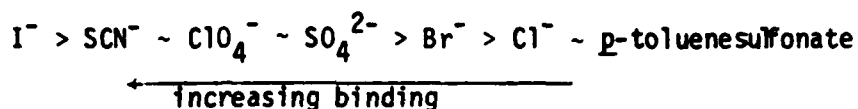
All of the transition metal complex anions are much more firmly bound than these anions. The relative binding spans a range of only about a factor of ten from I^- to Cl^- in the sense that a solution containing ~10/1 Cl^-/I^- will give a polymer having a ~1/1 Cl^-/I^-. In the same sense, $IrCl_6^{2-}$ to SO_4^{2-} spans a range of 10^3-10^4 in that ~20 $\mu\underline{M}$ K_2IrCl_6/0.1 $\underline{M}$ K_2SO_4 yields a polymer having ~1/1 $SO_4^{2-}/IrCl_6^{2-}$.

Given the results of others concerning the electrostatic binding of transition metal complexes to surface-confined polyions, the rather strong binding of the transition metal complexes to $(PQ^{2+})_n$ is not surprising.[13] For the weakly bound ions we find that the ions are very labile. Even the strongest of the weakest surface-confined ions, I^- is labile. Cyclic voltammetry signals apparently associated with $3I^- \rightleftharpoons I_3^-$ for $Pt/(PQ^{2+}\cdot 2I^-)_n$ electrodes immersed in 0.1 $\underline{M}$ KCl last for only a few scans at 100 mV/s, whereas the tightly bound metal complexes give rise to persistent cyclic voltammetry signals. The cyclic voltammetry (100 mV/s) for $(PQ^{2+/+\cdot})_n$ is not significantly dependent on the supporting electrolyte (0.1 $\underline{M}$) when a weakly bound anion is used. Thus, a wide range of K^+ or Na^+ salts are useful as the electrolyte for the $(PQ^{2+/+\cdot})_n$-coated electrodes. Only when the anion is strongly bound do we observe adverse effects on the kinetics of the $(PQ^{2+/+\cdot})_n$ redox system.

Summary

Electrochemical and Auger spectroscopic data establish a wide range of relative binding of anions to surfaces functionalized with $(PQ^{2+})_n$. Large, substitution inert, anionic transition metal complexes such as $IrCl_6^{2-/3-}$, $Fe(CN)_6^{3-/4-}$, $Ru(CN)_6^{3-/4-}$, $Mo(CN)_8^{3-/4-}$, and $Co(CN)_6^{3-}$ have all been found to be tightly bound against anions such as I^-, Br^-, Cl^-, SCN^-, ClO_4^-, SO_4^{2-}, or p-toluenesulfonate. The thermodynamically weakly bound anions are labile, rapidly displaced, and do not significantly alter the kinetics for the $(PQ^{2+/+\cdot})_n$ redox system. The strongly bound anions are not kinetically labile and do adversely affect the kinetics for the $(PQ^{2+/+\cdot})_n$ system. The correlation of the relative binding of $IrCl_6^{2-}$ vs. SO_4^{2-} using electrochemical and Auger detection establishes Auger to be a reliable and useful technique to determine the surface elemental composition of electrode surfaces modified with the $(PQ^{2+})_n$ system. The electrochemical data support the conclusion that the capacity of the $(PQ^{2+})_n$-coated electrodes to bind transition metal complexes is determined by the number of PQ^{2+} centers and the charge on the complex. Generally, complex anions can be bound to an extent that reflects complete charge compensation of the polyion bound to the surface. Finally, thermodynamics, not kinetics, has been shown to control the distribution of anions present in the surface bound $(PQ^{2+})_n$ when the electrolyte includes two or more anions.

References

1. Oyama, N.; Anson, F.C. J. Electrochem. Soc., 1980, 127, 247; Anal. Chem., 1980, 52, 1192.

2. Shigehara, K.; Oyama, N.; Anson, F.C. Inorg. Chem., 1981, 20, 518.

3. Oyama, N.; Sato, K.; Matsuda, H. J. Electroanal. Chem., 1980, 115, 149.

4. Rubinstein, I.; Bard, A.J. J. Am. Chem. Soc., 1980, 102, 6641.

5. (a) Schroeder, A.H.; Kaufman, F.B. J. Electroanal. Chem., 1980, 113, 209; (b) Schroeder, A.H.; Kaufman, F.B.; Patel, V.; Engler, E.M. J. Electroanal. Chem., 1980, 113, 193; (c) Kaufman, F.B.; Schroeder, A.H.; Engler, E.M.; Kramer, S.R.; Chambers, J.Q. J. Am. Chem. Soc., 1980, 102, 483.

6. Oyama, N.; Anson, F.C. J. Am. Chem. Soc., 1979, 101, 739, 3450; J. Electrochem. Soc., 1980, 127, 640.

7. Wrighton, M.S.; Palazzotto, M.C.; Bocarsly, A.B.; Bolts, J.M.; Fischer, A.B.; Nadjo, L. J. Am. Chem. Soc., 1978, 100, 7264.

8. Murray, R.W. Accs. Chem. Res., 1980, 13, 135.

9. Factor, A.; Rouse, T.O. J. Electrochem. Soc., 1980, 127, 1313.

10. Bookbinder, D.C.; Wrighton, M.S. J. Am. Chem. Soc., 1980, 102, 5123.

11. (a) Bookbinder, D.C.; Bruce, J.A.; Dominey, R.N.; Lewis, N.S.; Wrighton, M. S. Proc. Natl. Acad. Sci., U.S.A., 1980, 77, 6280; (b) Dominey, R.N.; Lewis, N. S.; Bruce, J.A.; Bookbinder, D.C.; Wrighton, M.S. J. Am. Chem. Soc., 1981, 103, 0000.

12. Moses, P.R.; Murray, R.W. J. Am. Chem. Soc., 1976, 98, 7435.

13. Lenhard, J.R.; Murray, R.W. J. Electroanal. Chem., 1977, 78, 195.

14. (a) Palmberg, P.W. J. Vac. Sci. Technol., 1972, 9, 160; (b) Holloway, D.M. ibid., 1975, 12, 392.

15. Davis, L.E.; MacDonald, N.C.; Palmberg, P.W.; Riach, G.E.; Weber, R.G. "Handbook of Auger Electron Spectroscopy", 2nd ed., Physical Electronics Division, Perkin-Elmer Corp., Eden Prairie, MN, 1976.

16. (a) Chang, C.C. Surf. Sci., 1971, 25, 53; (b) Van Oostrom, A. J. Vac. Sci. Technol., 1976, 13, 224.

17. Noufi, R.; Tench, D.; Warren, L.F. J. Electrochem. Soc., 1980, 127, 2709.

Table I. Concentration Dependence of Electrostatic Binding of $IrCl_6^{3-}$ to $Pt/(PQ^{2+} \cdot {}_xIrCl_6^{3-} + (1-x)SO_4^{2-})_n$ in 0.1 M K_2SO_4.

Electrode[a]	$[K_2IrCl_6]$[b]	$(PQ^{2+})_n + e^- \to (PQ^{+\cdot})_n$		$IrCl_6^{2-} + e^- \to IrCl_6^{3-}$		x
		E°, V vs. SCE[c]	Coverage, mol/cm²[d]	E°, V vs. SCE[c]	Coverage, mol/cm²[d]	
(a)	50 μM	-0.54	7.3×10^{-9}	+0.66	5.1×10^{-9}	1.0
	0	-0.51	7.3×10^{-9}	---	---	0.0
(b)	25 μM	-0.53	7.3×10^{-9}	+0.66	3.9×10^{-9}	0.8
	0	-0.51	7.3×10^{-9}	---	---	0.0
(c)	5.0 μM	-0.53	5.0×10^{-9}	+0.68	1.8×10^{-9}	0.5
	0	-0.51	5.0×10^{-9}	---	---	0.0
(d)	2.5 μM	-0.53	7.6×10^{-9}	+0.69	1.1×10^{-9}	0.2
	0	-0.51	7.6×10^{-9}	---	---	0.0
(e)	1.0 μM	-0.53	7.6×10^{-9}	+0.68	0.5×10^{-9}	0.1
	0	-0.51	7.6×10^{-9}	---	---	0.0

[a] Electrodes (a)-(e) are those characterized by the cyclic voltammetry scans in Figure 1, (a)-(e), respectively. Each electrode is thus an independent experiment.

[b] Bulk solution (~25 mT) concentration.

[c] Average position of the oxidation and reduction current peak for the surface confined species.

[d] Coverage of electrochemically active material from integration of cyclic voltammetry wave divided by electrode area. Note that the $IrCl_6^{2-/3-}$ is actually bound as $IrCl_6^{3-}$ since the electrode is held between $E°(PQ^{2+/+})_n$ and $E°(IrCl_6^{2-/3-})$; cf. text. Coverages are ±10%; error is due to inability to accurately subtract background currents.

Table II. Electrochemical Potential of Aqueous and Electrostatically Bound Complex Anions.

Complex	$E°$, V vs. SCE[a]	
	Solution	Bound to $(PQ^{2+})_n$
$Fe(CN)_6^{3-/4-}$	$+0.19 \pm 0.02$	$+0.20 \pm 0.03$
$Ru(CN)_6^{3-/4-}$	$+0.70 \pm 0.02$	$+0.68 \pm 0.03$
$Mo(CN)_8^{3-/4-}$	$+0.57 \pm 0.02$	$+0.60 \pm 0.03$
$IrCl_6^{2-/3-}$	$+0.65 \pm 0.02$	$+0.66 \pm 0.03$

[a]Electrochemical potentials, $E°$, for the indicated couple dissolved in H_2O at 25°C or confined to $(PQ^{2+})_n$ measured for Pt electrodes in 0.1 $\underline{M}$ KCl by cyclic voltammetry. The $E°$ is taken to be the average of the anodic and cathodic current peaks at a scan rate of 100 mV/s. The coverage of $(PQ^{2+})_n$ is generally in the range 5×10^{-9} - 5×10^{-8} mol/cm^2.

Table III. Electrochemical Experimentation to Establish Ordering of Binding of Complex Anions to $(PQ^{2+})_n$.

Experiment #	Perturbation	Response	Conclusion
1	Dip $(PQ^{2+}\cdot 2Cl^-)_n$ electrode into 0.1 M KCl/50 $\mu\underline{M}$ K_2IrCl_6.	$(PQ^{2+/+\cdot})_n$ wave broadens and shifts negative; $IrCl_6^{2-/3-}$ wave grows in until equal in area of $(PQ^{2+/+\cdot})_n$.	$IrCl_6^{2-} >> Cl^-$
2	Add $K_4Fe(CN)_6$ to 50 $\mu\underline{M}$ in above system.	$IrCl_6^{2-/3-}$ wave disappears; $Fe(CN)_6^{3-/4-}$ wave grows to ½ of $(PQ^{2+/+\cdot})_n$ wave.	$Fe(CN)_6^{4-} > IrCl_6^{2-}$
3	Add $K_4Mo(CN)_8$ to 50 $\mu\underline{M}$ in above system.	$Fe(CN)_6^{3-/4-}$ wave disappears; $Mo(CN)_8^{3-/4-}$ wave appears and grows to ½ of $(PQ^{2+/+\cdot})_n$ waves.	$Mo(CN)_8^{4-} > Fe(CN)_6^{4-}$
4	Add $K_4Ru(CN)_6$ to 50 $\mu\underline{M}$ in above system.	No change in cyclic voltammograms.	$Ru(CN)_6^{4-} < Mo(CN)_8^{4-}$
5	Dip electrode from 4 into saturated KCl for 5 min and scan in 0.1 M KCl containing no other ions.	Original response of $(PQ^{2+/+\cdot})_n$ regenerated; no signals detectable for bound complexes.	$(PQ^{2+}\cdot 2Cl^-)_n$ regenerated by ion exchange with excess Cl^-.
6	Dip $(PQ^{2+}\cdot 2Cl^-)_n$ electrode into 0.1 $\underline{M}$ KCl/50 $\mu\underline{M}$ each of $K_4Fe(CN)_6$, $K_4Ru(CN)_6$, K_2IrCl_6, $K_4Mo(CN)_8$.	$(PQ^{2+/+\cdot})_n$ wave broadened and shifted negative; eventual growth of $Mo(CN)_8^{3-/4-}$ to an area of ½ of $(PQ^{2+/+\cdot})_n$ wave.	Binding of $Mo(CN)_8^{4-}$ unaffected by presence of other complexes.
7	Dip $(PQ^{2+}\cdot 2Cl^-)_n$ electrode into 0.1 $\underline{M}$ KCl/50 $\mu\underline{M}$ K_2IrCl_6/50 $\mu\underline{M}$ $K_4Fe(CN)_6$.	$(PQ^{2+/+\cdot})_n$ wave broadens and shifts negative; waves for $Fe(CN)_6^{3-/4-}$ and $IrCl_6^{2-/3-}$ initially grow; eventually wave for $IrCl_6^{2-/3-}$ vanishes and $Fe(CN)_6^{3-/4-}$ grows to ½	Initial response kinetically controlled; eventual response thermodynamically controlled: $Fe(CN)_6^{4-} > IrCl_6^{2-}$

Table III. (Continued)

Experiment #	Perturbation	Response	Conclusion
8	Dip $(PQ^{2+} \cdot \frac{1}{2}Fe(CN)_6^{4-})_n$ electrode into 0.1 $\underline{M}$ KCl/50 $\mu\underline{M}$ $K_4Fe(CN)_6$/50 $\mu\underline{M}$ $K_3Co(CN)_6$.	Wave for $Fe(CN)_6^{3-/4-}$ declines to a value reflecting 70% loss of $Fe(CN)_6^{3-/4-}$.	$Co(CN)_6^{3-} > Fe(CN)_6^{4-}$
9	Dip $(PQ^{2+} \cdot 2Cl^-)_n$ electrode into 0.1 $\underline{M}$ KCl/50 $\mu\underline{M}$ $K_4Fe(CN)_6$.	$Fe(CN)_6^{3-/4-}$ wave grows to an area of ½ of that for $(PQ^{2+/+\cdot})_n$. $(PQ^{2+/+\cdot})_n$ wave broadens and shifts more negative.	$Fe(CN)_6^{4-} >> Cl^-$
10	Dip $(PQ^{2+} \cdot 2Cl^-)_n$ electrode into 0.1 $\underline{M}$ KCl/50 $\mu\underline{M}$ $K_4Fe(CN)_6$/50 $\mu\underline{M}$ $K_3Co(CN)_6$.	Same cyclic voltammetry as in #8.	$Co(CN)_6^{3-} > Fe(CN)_6^{4-}$

Table IV. Auger Signal Intensities for Anions Bound in $(PQ^{2+})_n$. [a]

Solution[b]	Signal Intensities, ±30%[c]	Conclusion
0.1 M KCl	Cl/C = 0.67	Cl⁻ Bound
0.01 M K₂IrCl₆	Cl/C = 1.4	IrCl₆²⁻ Bound
0.1 M KI	I/C ≈ 1.1 (0 signal interferes)[d]	I⁻ Bound
0.10 M K₂SO₄	S/C = 0.32	SO₄²⁻ Bound
0.05 M Na[p-toluenesulfonate]	S/C = 0.22; Cl/C = 0.20	p-toluenesulfonate ≈ Cl⁻
0.05 M KCl		
0.05 M KCl / 0.05 M KBr	Br/C = 0.13; Cl/C = 0.09	Br⁻ > Cl⁻
0.05 M KCl / 0.05 M KI	I/C ≈ 0.6[d]; Cl/C = 0.02	I⁻ > Br⁻ > Cl⁻
0.09 M KCl / 0.01 M KI	I/C ≈ 0.5[d]; Cl/C = 0.28	I⁻ > Cl⁻ (factor of ~10)
0.05 M KCl / 0.05 M KSCN	S/C = 0.45; Cl/C = 0.02	SCN⁻ > Cl⁻
0.05 M KSCN / 0.05 M KI	S/C = 0.29; I/C ≈ 0.3[d]	SCN⁻ ≈ I⁻
0.01 M KSCN / 0.01 M NaClO₄	S/C = 0.27; Cl/C = 0.59	ClO₄⁻ ≈ SCN⁻
0.05 M KCl / 0.05 M K₂SO₄	S/C = 0.30; Cl/C = 0.04	SO₄²⁻ > Cl⁻
0.05 M KBr / 0.05 M K₂SO₄	S/C = 0.16; Br/C = 0.10	SO₄²⁻ ≈ Br⁻
0.05 M KI / 0.05 M K₂SO₄	S/C ≈ 0.65; I/C ≈ 0.6[d]	I⁻ > SO₄²⁻

Table IV. (Continued)

Solution[b]	Signal Intensities, ±30%[c]	Conclusion
0.01 $\underline{M}$ K$_2$SO$_4$ 0.01 $\underline{M}$ NaClO$_4$ }[e]	S/C = 0.16; Cl/C = 0.16	SO$_4^{2-}$ ≈ ClO$_4^{-}$
1 m$\underline{M}$ K$_2$SO$_4$ 1 m$\underline{M}$ K$_2$PtCl$_6$ }	S/C - noise[f]; Cl/C = 0.87	PtCl$_6^{2-}$ >> SO$_4^{2-}$
0.10 $\underline{M}$ K$_2$SO$_4$ }[g] 50 $\mu\underline{M}$ K$_2$IrCl$_6$ }	S/C - noise[f]; Cl/C = 0.78	IrCl$_6^{2-}$ >> SO$_4^{2-}$

[a] Signal intensities (peak-to-peak height) are all relative to the C (272 eV) signal and are taken from depth profile analyses like those depicted in Figure 4. Data are from a portion of the depth profile where element ratios are the most constant.

[b] Aqueous solution (~25 ml) from which an electrode bearing $(PQ^{2+} \cdot 2Br^{-})_n$ (coverage in the range 5×10^{-9} to 5×10^{-8} mol/cm^2) was withdrawn after equilibration for 15 min at 25°C.

[c] Signals given are only those characteristic of the anion. Except where noted, there was no interference in the energy window used in the depth profile.

[d] The I signal and O signal near 503 eV interfere, but when I$^-$ is present the signal in this energy range is larger. The I$^-$ signal is characteristic because it has two peaks, whereas the O signal has only one.

[e] These data were recorded using a 3 KeV electron beam; all other data were recorded using a 5 KeV electron beam. This may cause some variability in the element ratios.

[f] No signal beyond background was detectable.

[g] These data are from an Auger spectrum without sputtering, cf. Figure 2.

Figure Captions

Figure 1. Cyclic voltammograms (100 mV/s) of a Pt/$(PQ^{2+})_n$ electrode in solutions containing 0.1 $\underline{M}$ K_2SO_4 and (a) 50 $\mu\underline{M}$ K_2IrCl_6, (b) 25 $\mu\underline{M}$ K_2IrCl_6, (c) 5.0 $\mu\underline{M}$ K_2IrCl_6, (d) 7.5 $\underline{M}$ K_2IrCl_6, and (e) 1.0 $\mu\underline{M}$ K_2IrCl_6. The coverage of electroactive $(PQ^{2+/+\cdot})_n$ is 7.6 x 10^{-9} moles/cm^2 for (a) and (b), 5.0 x 10^{-9} moles/cm^2 for (c) and 7.3 x 10^{-9} moles for (d) and (e). Cf. also Table I.

Figure 2. Auger spectra for Pt/$(PQ^{2+} \cdot \frac{2}{3} x \ IrCl_6^{3-} + (1 - x)SO_4^{2-})_n$ electrodes. In (a) the electrode was withdrawn from a solution containing 0.1 $\underline{M}$ K_2SO_4 and 1 $\mu\underline{M}$ K_2IrCl_6 and is the electrode characterized by cyclic voltammetry in Figure 1e. In (b) the electrode was withdrawn from a solution containing 0.1 $\underline{M}$ K_2SO_4 and 50 $\mu\underline{M}$ K_2IrCl_6 and is the electrode characterized by cyclic voltammetry in Figure 1a. Each electrode was washed with H_2O prior to the Auger and the surfaces were not sputtered. Note that the $IrCl_6^{3-}$, not $IrCl_6^{2-}$, is surface-confined, since the electrode was removed after electrochemical equilibration at a potential between $E°(PQ^{2+/+\cdot})_n$ and $E°(IrCl_6^{2-/3-})$.

Figure 3. A graph comparing electrochemical and Auger data for Pt/$(PQ^{2+} \cdot \frac{2}{3} x \ IrCl_6^{3-} + (1-x)SO_4^{2-})_n$ electrodes. The cyclic voltammetry of these electrodes is shown in Figure 1. The scale on the left hand side refers to the ratio of the integrated areas of the $IrCl_6^{2-/3-}$ and $(PQ^{2+/+\cdot})_n$ waves, in solutions containing the appropriate concentration of K_2IrCl_6 (X). The scale on the right hand side refers to the ratio of Auger signals obtained for C and Cl on these same electrodes (•) without sputtering. Auger spectra for $[IrCl_6^{2-}]$ = 1 $\mu\underline{M}$ and 50 $\mu\underline{M}$ are shown in Figure 2. Auger signal intensities have not been corrected for element sensitivity.

Figure 4. Auger/depth profile analysis of $Pt/(PQ^{2+} \cdot xIrCl_6^{2-} + (1 - x)SO_4^{2-})_n$ electrodes. The electrode characterized in (a) was withdrawn from a solution of 5 m$\underline{M}$ K_2IrCl_6 and that in (b) was withdrawn from a solution of 0.1 $\underline{M}$ K_2SO_4. In (a) $x \approx 1$ and in (b) $x \approx 0$. Electrodes were washed with H_2O prior to Auger analysis. Note that low energy Pt signals interfere with the low energy signals characteristic of other elements, especially S.

Figure 5. Cyclic voltammograms (100 mV/s) in 0.1 $\underline{M}$ KCl of electrode (a) a $Pt/(PQ^{2+} \cdot \frac{1}{2}Mo(CN)_8^{4-})_n$ electrode prepared by immersing a $Pt/(PQ^{2+})_n$ electrode into ~5 m$\underline{M}$ $K_4Mo(CN)_8/H_2O$, and then rinsing, and (b) at $Pt/(PQ^{2+} \cdot \frac{1}{2}Fe(CN)_6^{4-})_n$ electrode prepared as in (a) except using $K_4Fe(CN)_6$. The coverage of electroactive $(PQ^{2+/+})_n$ is 1.3×10^{-8} mol/cm^2 for (a) and 3.7×10^{-9} mol/cm^2 for (b).

Figure 6. Auger spectral analysis of $Pt/PQ^{2+} \cdot 2xCl^- \cdot \frac{1}{2}(1 - x)Fe(CN)_6^{4-})_n$. In (a) the electrode was withdrawn from 0.1 $\underline{M}$ KCl, 1 $\mu\underline{M}$ $K_4Fe(CN)_6$; $x \approx 1$ and in (b) the electrode was withdrawn from 0.1 $\underline{M}$ KCl, 100 $\mu\underline{M}$ $K_4Fe(CN)_6$; $x \approx 0$. Electrodes were washed prior to Auger analysis but were not sputtered.

Figure 7. Cyclic voltammograms for a $Pt/(PQ^{2+} \cdot \frac{1}{2}Mo(CN)_8^{4-})_n$ electrode in 0.1 $\underline{M}$ KCl/H_2O at different scan rates. The inset shows that the peak current for the $Mo(CN)_8^{4-/3-}$ wave varies linearly with the scan rate, as expected for a reversible, surface-attached species. The coverage of electroactive $(PQ^{2+})_n$ is 1×10^{-9} mol/cm^2.

Figure 8. Cyclic voltammograms, 100 mV/s, of a $Pt/(PQ^{2+})_n$ electrode in (a) ---- 0.1 $\underline{M}$ KCl; —— 0.1 $\underline{M}$ KCl/50 $\mu\underline{M}$ K_2IrCl_6; (b) 0.1 $\underline{M}$ KCl/50 $\mu\underline{M}$ K_2IrCl_6/50 $\mu\underline{M}$ $K_4Fe(CN)_6$; (c) 0.1 $\underline{M}$ KCl/50 $\mu\underline{M}$ K_2IrCl_6/50 $\mu\underline{M}$ $K_4Fe(CN)_6$/50 $\mu\underline{M}$ $K_4Mo(CN)_8$. The coverage of PQ^{2+} is 2.1×10^{-8} mol/cm^2. In each case the unpotentiostatted electrode was equilibrated for ~15 min prior to running the cyclic voltammogram.

Figure 9. Cyclic voltammograms, 100 mV/s, of a $Pt/(PQ^{2+})_n$ electrode in (a)
—— 0.1 $\underline{M}$ KCl; ---- 0.1 $\underline{M}$ KCl/50 $\mu\underline{M}$ $K_4Fe(CN)_6$; (b) —— 0.1 $\underline{M}$ KCl/50 $\mu\underline{M}$
$K_4Fe(CN)_6$/25 $\mu\underline{M}$ $K_3Co(CN)_6$; ---- 0.1 $\underline{M}$ KCl/50 $\mu\underline{M}$ $K_4Fe(CN)_6$; (c) —— 0.1 $\underline{M}$ KCl/
50 $\mu\underline{M}$ $K_4Fe(CN)_6$/50 $\mu\underline{M}$ $K_3Co(CN)_6$.   In (b) and (c) the cyclic voltammograms are
the same when starting with either $Pt/(PQ^{2+} \cdot 2Cl^-)_n$ or
$Pt/(PQ^{2+} \cdot \frac{1}{2}Fe(CN)_6{}^{4-})_n$.   The coverage of PQ^{2+} is 2.8 x 10^{-8} mol/cm^2.
As for Figure 8, the unpotentiostatted electrode was equilibrated for
~15 min prior to running the cyclic voltammogram.

a) 50 μM K₂IrCl₆

200 μA/cm²

b) 25 μM K₂IrCl₆

200 μA/cm²

c) 5.0 μM K₂IrCl₆

200 μA/cm²

d) 2.5 μM K₂IrCl₆

200 μA/cm²

e) 1.0 μM K₂IrCl₆

200 μA/cm²

CURRENT

anodic — 0 — cathodic

POTENTIAL, V vs SCE

-0.4   0   +0.4   +0.8

a) $Pt/(PQ^{2+} \cdot \frac{2}{3} x IrCl_6^{3-} \cdot (1-x)SO_4^{2-})_n$

$x \approx 0$

$\frac{dN}{dE}$

Si

S

Cl

N

O

C

b) $Pt/(PQ^{2+} \cdot \frac{2}{3} x IrCl_6^{3-} \cdot (1-x)SO_4^{2-})_n$

$x \approx 1$

$\frac{dN}{dE}$

Si

N

O

Cl

C

200   400   600

ELECTRON ENERGY, eV

a) $Pt/(PQ^{2+} \cdot IrCl_6^{2-})_n$

Pt (X2)
Cl (X1)
C (X1)
N (X2)
O (X1)
Si (X2)

b) $Pt/(PQ^{2+} \cdot SO_4^{2-})_n$

Pt (X2)
S (X2)
C (X1)
N (X2)
O (X1)
Si (X1)

Auger Peak-to-Peak Amplitude, Arbitrary Units

Sputtering Time, Minutes

a) $Pt/(PQ^{2+} \cdot 2xCl^{-} \cdot \frac{1}{2}(1-x)Fe(CN)_6^{4-})_n$

$x \approx 1$

Si Cl N O C Si Pt

$\frac{dN}{dE}$

b) $Pt/(PQ^{2+} \cdot 2xCl^{-} \cdot \frac{1}{2}(1-x)Fe(CN)_6^{4-})_n$

$x \approx 0$

Si Cl N O Fe C Si Pt

$\frac{dN}{dE}$

400   800   1200   1600

ELECTRON ENERGY, eV

a) Pt/(PQ^{2+})$_n$

0.1 $\underline{M}$ KCl

50 $\mu\underline{M}$ K$_2$IrCl$_6$
0.1 $\underline{M}$ KCl

50 μA

anodic

cathodic

0

b) 50 $\mu\underline{M}$ K$_2$IrCl$_6$, 50 $\mu\underline{M}$ K$_4$Fe(CN)$_6$, 0.1 $\underline{M}$ KCl

50 μA

anodic

cathodic

0

CURRENT

c) 50 $\mu\underline{M}$ K$_2$IrCl$_6$, 50 $\mu\underline{M}$ K$_4$Fe(CN)$_6$, 50 $\mu\underline{M}$ K$_4$Mo(CN)$_8$, 0.1 $\underline{M}$ KCl

50 μA

anodic

cathodic

0

-0.8   -0.4   0.0   +0.4   0.8

POTENTIAL, V vs. SCE

a) **Pt/(PQ²⁺)ₙ**

0.1 M KCl

50 μM K₄Fe(CN)₆
0.1 M KCl

100 μA

b)

—— 50 μM K₄Fe(CN)₆, 25 μM K₃Co(CN)₆
0.1 M KCl

- - - 50 μM K₄Fe(CN)₆
0.1 M KCl

100 μA

c)

—— 50 μM K₄Fe(CN)₆, 50 μM K₃Co(CN)₆
0.1 M KCl

- - - 50 μM K₄Fe(CN)₆
0.1 M KCl

100 μA

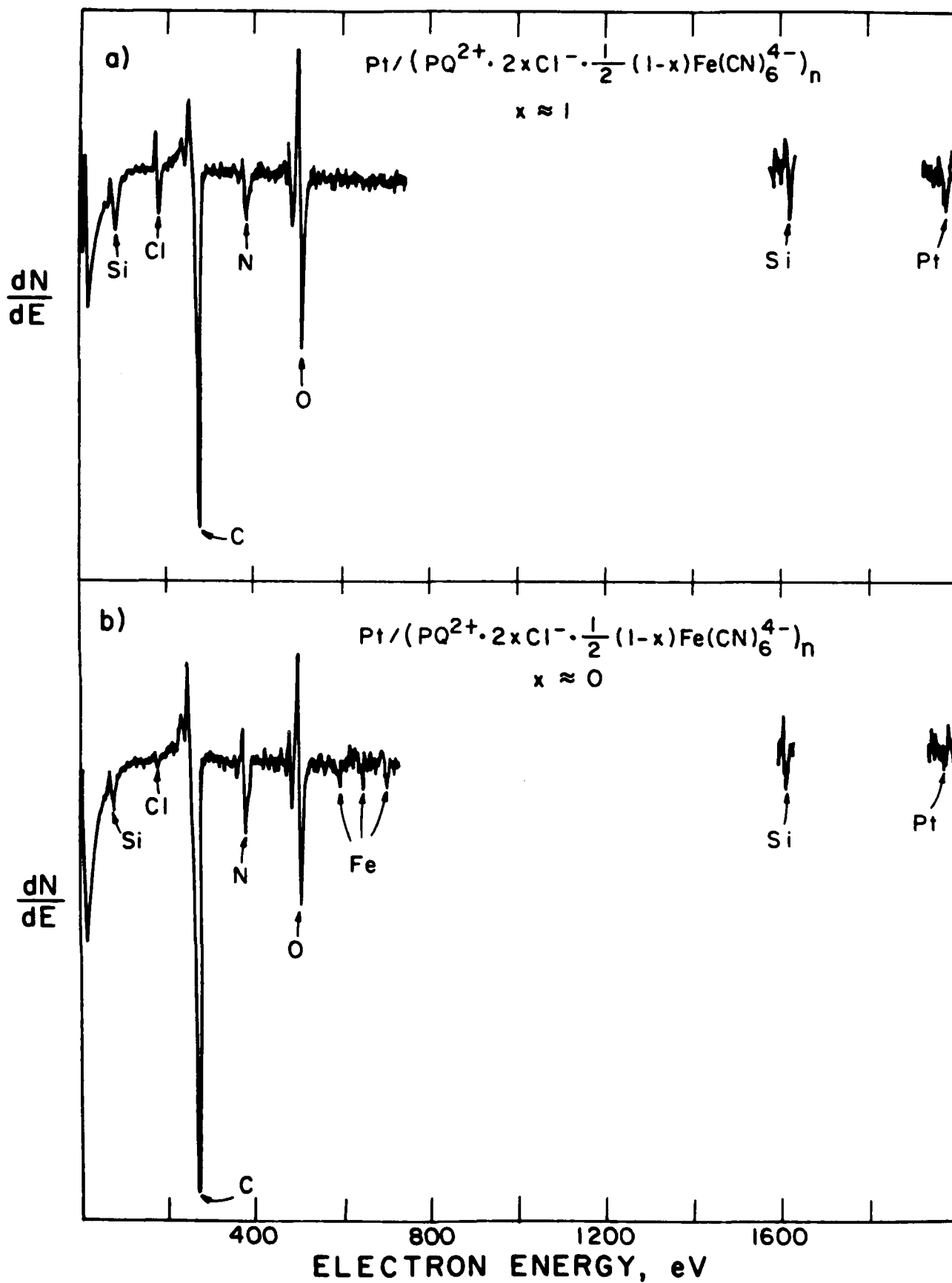CURRENT

cathodic 0 anodic

POTENTIAL, V vs SCE

-0.4   0.0   +0.4

TECHNICAL REPORT DISTRIBUTION LIST, 051A

	No. Copies		No. Copies
Dr. M. A. El-Sayed Department of Chemistry University of California, Los Angeles Los Angeles, California 90024	1	Dr. M. Rauhut Chemical Research Division American Cyanamid Company Bound Brook, New Jersey 08805	1
Dr. E. R. Bernstein Department of Chemistry Colorado State University Fort Collins, Colorado 80521	1	Dr. J. I. Zink Department of Chemistry University of California, Los Angeles Los Angeles, California 90024	1
Dr. C. A. Heller Naval Weapons Center Code 6059 China Lake, California 93555	1	Dr. D. Haarer IBM San Jose Research Center 5600 Cottle Road San Jose, California 95143	1
Dr. J. R. MacDonald Chemistry Division Naval Research Laboratory Code 6110 Washington, D.C. 20375	1	Dr. John Cooper Code 6130 Naval Research Laboratory Washington, D.C. 20375	1
Dr. G. B. Schuster Chemistry Department University of Illinois Urbana, Illinois 61801	1	Dr. William M. Jackson Department of Chemistry Howard University Washington, DC 20059	1
Dr. A. Adamson Department of Chemistry University of Southern California Los Angeles, California 90007	1	Dr. George E. Walraffen Department of Chemistry Howard University Washington, DC 20059	1
Dr. M. S. Wrighton Department of Chemistry Massachusetts Institute of Technology Cambridge, Massachusetts 02139	1		

TECHNICAL REPORT DISTRIBUTION LIST, 359

	No. Copies		No. Copies
Dr. A. B. Ellis Chemistry Department University of Wisconsin Madison, Wisconsin 53706	1	Dr. R. P. Van Duyne Department of Chemistry Northwestern University Evanston, Illinois 60201	1
Dr. M. Wrighton Chemistry Department Massachusetts Institute of Technology Cambridge, Massachusetts 02139	1	Dr. B. Stanley Pons Department of Chemistry University of Alberta Edmonton, Alberta CANADA T6G 2G2	1
Larry F. Plew Naval Weapons Support Center Code 30736, Building 2906 Crane, Indiana 47522	1	Dr. Michael J. Weaver Department of Chemistry Michigan State University East Lansing, Michigan 48824	1
S. Ruby DOE (STOR) 600 F Street Washington, D.C. 20545	1	Dr. R. David Rauh EIC Corporation 55 Chapel Street Newton, Massachusetts 02158	1
Dr. Aaron Wold Brown University Department of Chemistry Providence, Rhode Island 02192	1	Dr. J. David Margerum Research Laboratories Division Hughes Aircraft Company 3011 Malibu Canyon Road Malibu, California 90265	1
Dr. R. C. Chudacek McGraw-Edison Company Edison Battery Division Post Office Box 28 Bloomfield, New Jersey 07003	1	Dr. Martin Fleischmann Department of Chemistry University of Southampton Southampton S09 5NH England	1
Dr. A. J. Bard University of Texas Department of Chemistry Austin, Texas 78712	1	Dr. Janet Osteryoung Department of Chemistry State University of New York at Buffalo Buffalo, New York 14214	1
Dr. M. M. Nicholson Electronics Research Center Rockwell International 3370 Miraloma Avenue Anaheim, California	1	Dr. R. A. Osteryoung Department of Chemistry State University of New York at Buffalo Buffalo, New York 14214	1
Dr. Donald W. Ernst Naval Surface Weapons Center Code R-33 White Oak Laboratory Silver Spring, Maryland 20910	1	Mr. James R. Moden Naval Underwater Systems Center Code 3632 Newport, Rhode Island 02840	1

TECHNICAL REPORT DISTRIBUTION LIST, 359

	No. Copies		No. Copies
Dr. R. Nowak Naval Research Laboratory Code 6130 Washington, D.C. 20375	1	Dr. John Kincaid Department of the Navy Stategic Systems Project Office Room 901 Washington, DC 20376	1
Dr. John F. Houlihan Shenango Valley Campus Pennsylvania State University Sharon, Pennsylvania 16146	1	M. L. Robertson Manager, Electrochemical Power Sonices Division Naval Weapons Support Center	
Dr. M. G. Sceats Department of Chemistry University of Rochester Rochester, New York 14627	1	Crane, Indiana 47522 Dr. Elton Cairns Energy & Environment Division	1
Dr. D. F. Shriver Department of Chemistry Northwestern University Eva ston, Illinois 60201	1	Lawrence Berkeley Laboratory University of California Berkeley, California 94720 Dr. Bernard Spielvogel	1
Dr. D. H. Whitmore Department of Materials Science Northwestern University Evanston, Illinois 60201	1	U.S. Army Research Office P.O. Box 12211 Research Triangle Park, NC 27709	1
Dr. Alan Bewick Department of Chemistry The University Southampton, S09 5NH England	1	Dr. Denton Elliott Air Force Office of Scientific Research Bldg. 104 Bolling AFB Washington, DC 20332	1
Dr. A. Himy NAVSEA-5433 NC #4 2541 Jefferson Davis Highway Arlington, Virginia 20362	1		

TECHNICAL REPORT DISTRIBUTION LIST, 359

	No. Copies		No. Copies

Dr. Paul Delahay
Department of Chemistry
New York University
New York, New York 10003 — 1

Dr. E. Yeager
Department of Chemistry
Case Western Reserve University
Cleveland, Ohio 41106 — 1

Dr. D. N. Bennion
Department of Chemical Engineering
Brigham Young University
Provo, Utah 84602 — 1

Dr. R. A. Marcus
Department of Chemistry
California Institute of Technology
Pasadena, California 91125 — 1

Dr. J. J. Auborn
Bell Laboratories
Murray Hill, New Jersey 07974 — 1

Dr. Adam Heller
Bell Laboratories
Murray Hill, New Jersey 07974 — 1

Dr. T. Katan
Lockheed Missiles & Space
  Co, Inc.
P.O. Box 504
  Sunnyvale, California 94088 — 1

Dr. Joseph Singer, Code 302-1
NASA-Lewis
21000 Brookpark Road
Cleveland, Ohio 44135 — 1

Dr. S. Brummer
EIC Incorporated
55 Chapel Street
Newton, Massachusetts 02158 — 1

Library
P. R. Mallory and Company, Inc.
Northwest Industrial Park
Burlington, Massachusetts 01803 — 1

Dr. P. J. Hendra
Department of Chemistry
University of Southhampton
Southhampton SO9 5NH
United Kingdom — 1

Dr. Sam Perone
Department of Chemistry
Purdue University
West Lafayette, Indiana 47907 — 1

Dr. Royce W. Murray
Department of Chemistry
University of North Carolina
Chapel Hill, North Carolina 27514 — 1

Naval Ocean Systems Center
Attn: Technical Library
San Diego, California 92152 — 1

Dr. C. E. Mueller
The Electrochemistry Branch
Materials Division, Research
  & Technology Department
Naval Surface Weapons Center
White Oak Laboratory
Silver Spring, Maryland 20910 — 1

Dr. G. Goodman
Globe-Union Incorporated
5757 North Green Bay Avenue
Milwaukee, Wisconsin 53201 — 1

Dr. J. Boechler
Electrochimica Corporation
Attention: Technical Library
2485 Charleston Road
Mountain View, California 94040 — 1

Dr. P. P. Schmidt
Department of Chemistry
Oakland University
Rochester, Michigan 48063 — 1

Dr. H. Richtol
Chemistry Department
Rensselaer Polytechnic Institute
Troy, New York 12181 — 1

TECHNICAL REPORT DISTRIBUTION LIST, GEN

	No. Copies		No. Copies
Office of Naval Research Attn: Code 472 800 North Quincy Street Arlington, Virginia 22217	2	U.S. Army Research Office Attn: CRD-AA-IP P.O. Box 1211 Research Triangle Park, N.C. 27709	1
ONR Branch Office Attn: Dr. George Sandoz 536 S. Clark Street Chicago, Illinois 60605	1	Naval Ocean Systems Center Attn: Mr. Joe McCartney San Diego, California 92152	1
~~ONR Area Office~~ ~~Attn:~~ ~~Dr. Established.~~ ~~715 Broadway~~ ~~New York, New York 10003~~	1	Naval Weapons Center Attn: Dr. A. B. Amster, Chemistry Division China Lake, California 93555	1
ONR Western Regional Office 1030 East Green Street Pasadena, California 91106	1	Naval Civil Engineering Laboratory Attn: Dr. R. W. Drisko Port Hueneme, California 93401	1
ONR Eastern/Central Regional Office Attn: Dr. L. H. Peebles Building 114, Section D 665 Summer Street Boston, Massachusetts 02210	1	Department of Physics & Chemistry Naval Postgraduate School Monterey, California 93940	1
Director, Naval Research Laboratory Attn: Code 6100 Washington, D.C. 20390	1	Dr. A. L. Slafkosky Scientific Advisor Commandant of the Marine Corps (Code RD-1) Washington, D.C. 20380	1
The Assistant Secretary of the Navy (RE&S) Department of the Navy Room 4E736, Pentagon Washington, D.C. 20350	1	Office of Naval Research Attn: Dr. Richard S. Miller 800 N. Quincy Street Arlington, Virginia 22217	1

Commander, Naval Air Systems Command
Attn: Code 310C (H. Rosenwasser)
Department of the Navy
Washington, D.C. 20360
	1	Naval Ship Research and Development
		  Center
		Attn: Dr. G. Bosmajian, Applied
		  Chemistry Division
		Annapolis, Maryland 21401
			1

Defense Technical Information Center Building 5, Cameron Station Alexandria, Virginia 22314	12	Naval Ocean Systems Center Attn: Dr. S. Yamamoto, Marine Sciences Division San Diego, California 91232	1
Dr. Fred Saalfeld Chemistry Division, Code 6100 Naval Research Laboratory Washington, D.C. 20375	1	Mr. John Boyle Materials Branch Naval Ship Engineering Center Philadelphia, Pennsylvania 19112	1

TECHNICAL REPORT DISTRIBUTION LIST, GEN

<u>No.</u>
<u>Copies</u>

Dr. Rudolph J. Marcus
Office of Naval Research
Scientific Liaison Group
American Embassy
APO San Francisco 96503   1

Mr. James Kelley
DTNSRDC Code 2803
Annapolis, Maryland 21402   .   1